Chapter 3

Hydrogen Spillover in Platinum-Doped Superactivated Carbon

3.1 Overview

Effective storage of hydrogen by physisorbent materials has remained limited to cryogenic temperatures since hydrogen binding interactions are not significantly larger than the average thermal energy at 298 K: typically 4-6 kJ (mol H_2)$^{-1}$. The excess adsorption capacities of known materials are less than 10 mmol g^{-1} (2 wt%), and less than 5 mmol g^{-1} in all but a few select cases. These figures do not include the added mass of the storage vessel and delivery apparatus, and are far from the targets suggested by the DOE for mobile vehicle applications. The volumetric density enhancement from hydrogen adsorption at room temperature has also not been shown to be significant enough to overcome the penalty in mass of including the sorbent.

It was proposed that an enhancement of the hydrogen storage capacities of physisorptive materials can be gained by hydrogen spillover from a metal catalyst onto the adsorbing surface.[1-7] Hydrogen spillover is dissociative chemisorption of dihydrogen onto a metal particle followed by migration of hydrogen atoms onto the surface of the bulk material and subsequent diffusion away from the receptor site,[8-10] as shown in

Figure 3.1. Platinum, palladium, and nickel have been studied as metal catalysts for spillover, while materials including zeolites, metal-organic frameworks (MOFs), and carbons were used as host materials.

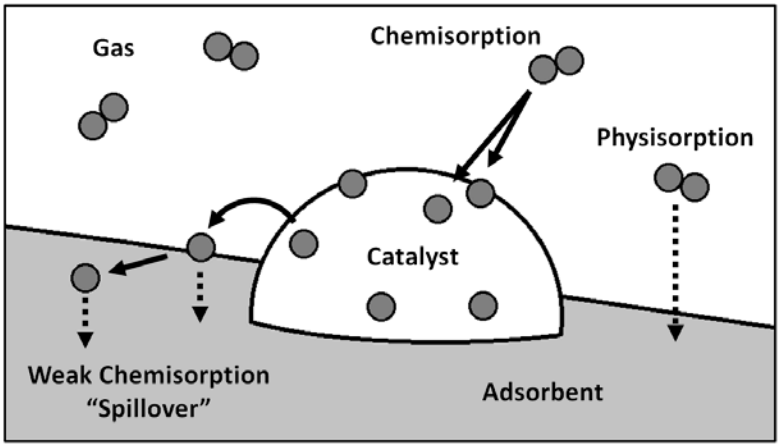

Figure 3.1. Spillover of the dissociated atoms of a diatomic molecule following chemisorption at the site of a catalyst particle, onto the surface of the support material.

The spillover concept is well documented in heterogeneous catalysis,[10] but has only recently been studied as a hydrogen storage mechanism. Reports of remarkable increases in hydrogen uptake for these systems have generated much further research, even toward enhancing contact between the metal sites and the substrate surface via carbonized "bridges".[4] However, the details of hydrogen spillover are not understood. This is partly because of the challenging task of detecting atomic hydrogen in spillover systems and partly because of the inherent difficulties in accurately measuring small changes in hydrogen uptake at room temperature. Although direct observation of atomic hydrogen has been recently demonstrated by transmission electron microscopy on a single graphene sheet,[11] volumetric measurements of hydrogen uptake are never this sensitive. Investigations using inelastic neutron scattering also recently yielded

evidence of the formation of new C-H bonds on the surface of activated carbon fibers after spillover from palladium clusters; however, reversibility was unclear and enhancement attributed to spillover was not tested at high pressures.[5] Interestingly, theoretical models cannot account for the remarkable enhancement of hydrogen uptake capacity in carbon materials due to spillover reported by experimental investigation.[5, 12-14]

In the present study, the hydrogen spillover effect was tested in the simplest experimental system. Platinum nanoparticles directly dispersed on high surface area superactivated carbon were used as the metal receptor sites for hydrogen dissociation. Platinized carbon was the standard system studied in the discovery of the spillover phenomenon,[8] the benzene hydrogenation experiments that later confirmed the spillover mechanism,[9] and in the first reports of spillover enhancement to hydrogen storage capacity.[1, 2] Platinum metal does not form a bulk hydride phase and therefore only surface chemisorption is expected (unlike palladium where absorbed hydrogen is a complication). While “bridging” is reported to increase hydrogen uptake by spillover,[4] this phenomenon is not essential for spillover to occur and was not the topic of this study. A commercially available superactivated carbon (Maxsorb MSC-30) was selected for its close similarity to AX-21, a high surface area carbon material previously used in spillover experiments. Hydrogen uptake isotherms of the platinum containing samples (Pt-MSC-30) were measured at room temperature (296 K), where spillover is expected. Synthesis and adsorption experiments were carried out in the most straightforward and standard way for corroborating the effect, following the steps reported by Li and Yang.[3]

In all 0.2 g samples, the size used in previous spillover studies, H_2 uptake was not substantially above instrumental background as measured by standard volumetric techniques. In experiments using a larger sample (>3 g), specific excess hydrogen uptake in Pt-MSC-30 was well above background, but was found to be less than in unmodified MSC-30 at high pressures.

3.2 Materials Processing and Synthesis

3.2.1 MSC-30 and AX-21

Maxsorb MSC-30 superactivated carbon was obtained from Kansai Coke & Chemicals Company, since it is a suitable support material for catalyst nanoparticles, essentially equivalent to AX-21 (from Anderson Development Co.) previously used in spillover experiments.[3] Both materials are produced by activation of petroleum coke with molten KOH, using a process patented by Standard Oil Company (later, Amoco Corporation).[15] Both have a surface area near 3000 m^2g^{-1}, exhibit similar chemical character and textural morphology, and are classified as "superactivated" or "AX-21 type" carbon.[16] The oxygen content of superactivated carbon, a characteristic which may be important to the hydrogen spillover mechanism,[17] is proportional to the BET surface area and is expected to be similar for both materials.[18]

3.2.2 Synthesis Methods

Maxsorb MSC-30 superactivated carbon (obtained from Kansai Coke & Chemicals Company, Ltd.) was stored at 393 K under vacuum in a Buchi glass oven. The Pt-MSC-30 samples were prepared by incipient wetness impregnation, in an analogous method as

for Pt/AX-21.[3] For each sample, 200 mg of dried MSC-30 was dispersed in acetone and magnetically stirred for 30 min at room temperature. A 2 mL solution consisting of 50 mg H_2PtCl_6 in acetone was then added dropwise to the stirring MSC-30 solution over 5 min. The slurry was removed and placed in an ultrasonic bath (50 W, 42 kHz, 1.9 L capacity) for 60 min and then magnetically stirred at room temperature for 24 h. The acetone was evaporated by heating the sample at 333 K for 12 h. The dry mixture was transferred to a ceramic boat and immediately placed in He flow inside a horizontal quartz tube furnace to prevent moisture uptake. The furnace was pre-heated to 393 K and held for 2 h under constant He flow. For reduction, the gas flow was switched to H_2 and the furnace was heated to 573 K and held for 2 h. The flow was again returned to He and the furnace allowed to cool to room temperature over 30 min. Each sample (~0.2 g) was sealed in a glass vial in Ar atmosphere and stored in a glovebox. A large number of 0.2 g Pt-MSC-30 samples (~40) were prepared and then combined to achieve sample sizes up to 3.2 g. Adapting the synthesis procedures of Pt/AX-21[3] to make large sample sizes required the use of multiple ceramic boats placed in a large diameter (5 cm) tube furnace. Sample characterization was undertaken to assure that individual syntheses yielded consistent products before combining them. Prior to hydrogen adsorption, the samples were degassed in vacuum at 623 K for 12 h. Sample mass, measured in the degassed state, was varied from 0.2-3.4 g for isotherm experiments of Pt-MSC-30 and pure MSC-30.

3.3 Materials Characterization

3.3.1 Nitrogen Adsorption

Nitrogen isotherms were measured at 77 K for MSC-30 and Pt-MSC-30. These measurements were made with a Micromeritics ASAP 2420 and surface areas were calculated using the BET method as implemented by Micromeritics ASAP 2420 version 2.02 software. The BET surface areas of MSC-30 and Pt-MSC-30 were measured to be 3420 m^2g^{-1} and 2810 m^2g^{-1}, respectively. The surface area of MSC-30 is larger than that of Anderson AX-21, reported as 2880 m^2g^{-1}.[3] The decrease in surface area of MSC-30 upon adding Pt nanoparticles is consistent with the reported data for AX-21. This can be explained by Pt particles blocking or filling pores in the superactivated carbon.

3.3.2 X-Ray Diffraction

X-ray diffraction (XRD) experiments were performed using a PANalytical X'Pert Pro powder diffractometer with Cu $K\alpha_{1,2}$ radiation. Diffraction patterns of MSC-30 and

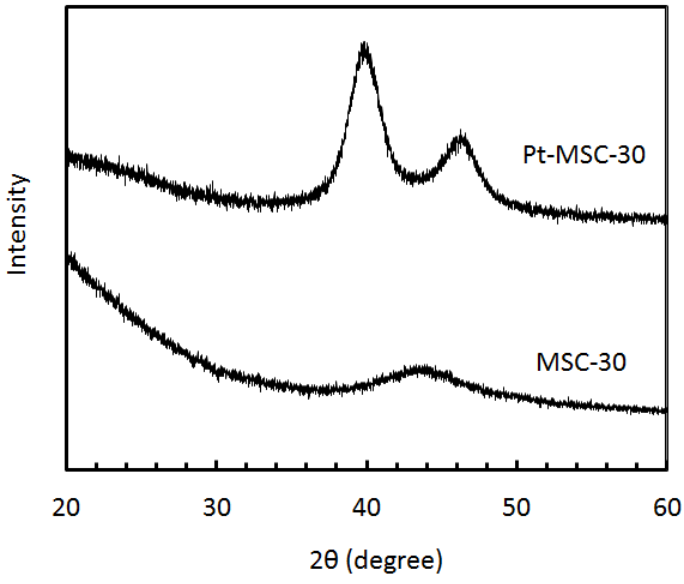

Figure 3.2. XRD patterns of Pt-MSC-30 and unmodified MSC-30.

Pt-MSC-30 are shown in Figure 3.2. The broad peak centered at 2ϑ = 43° for pure MSC-30 is consistent with that reported for AX-21. The peaks in the Pt-MSC-30 pattern at 2ϑ = 39.9° and 46.4° are the (111) and (200) reflections of the cubic platinum crystal structure. No platinum oxide peaks were detected, suggesting fully reduced Pt metal nanoparticles in the sample. From the widths of the diffraction peaks, the mean crystallite diameter was calculated with the Scherrer equation to be 3.6 nm (using the Scherrer constant K = 0.83 for spherical particles).[19]

3.3.3 Transmission Electron Microscopy

High resolution transmission electron microscopy (TEM) images were collected on a Tecnai TF30 operated at 300 keV. Scanning transmission electron microscopy (STEM) images were acquired with a high angle annular dark field (HAADF) detector. Samples were prepared for TEM by dispersing a finely ground mixture of Pt-MSC-30 and isopropanol on a holey carbon grid. TEM studies on Pt-MSC-30 showed a distribution in size of Pt particles from 2-10 nm in diameter, consistent with the 7 nm size from the Scherrer equation. TEM images at three magnifications are shown in Figure 3.3. The nanoparticles were highly dispersed on the surface of the activated carbon in all areas examined. This was further verified by HAADF microscopy, where intensity is proportional to Z^2 (Z is atomic number); platinum scatters electrons much more strongly than the carbon support and was readily observed in the form of small nanoparticles throughout the material.

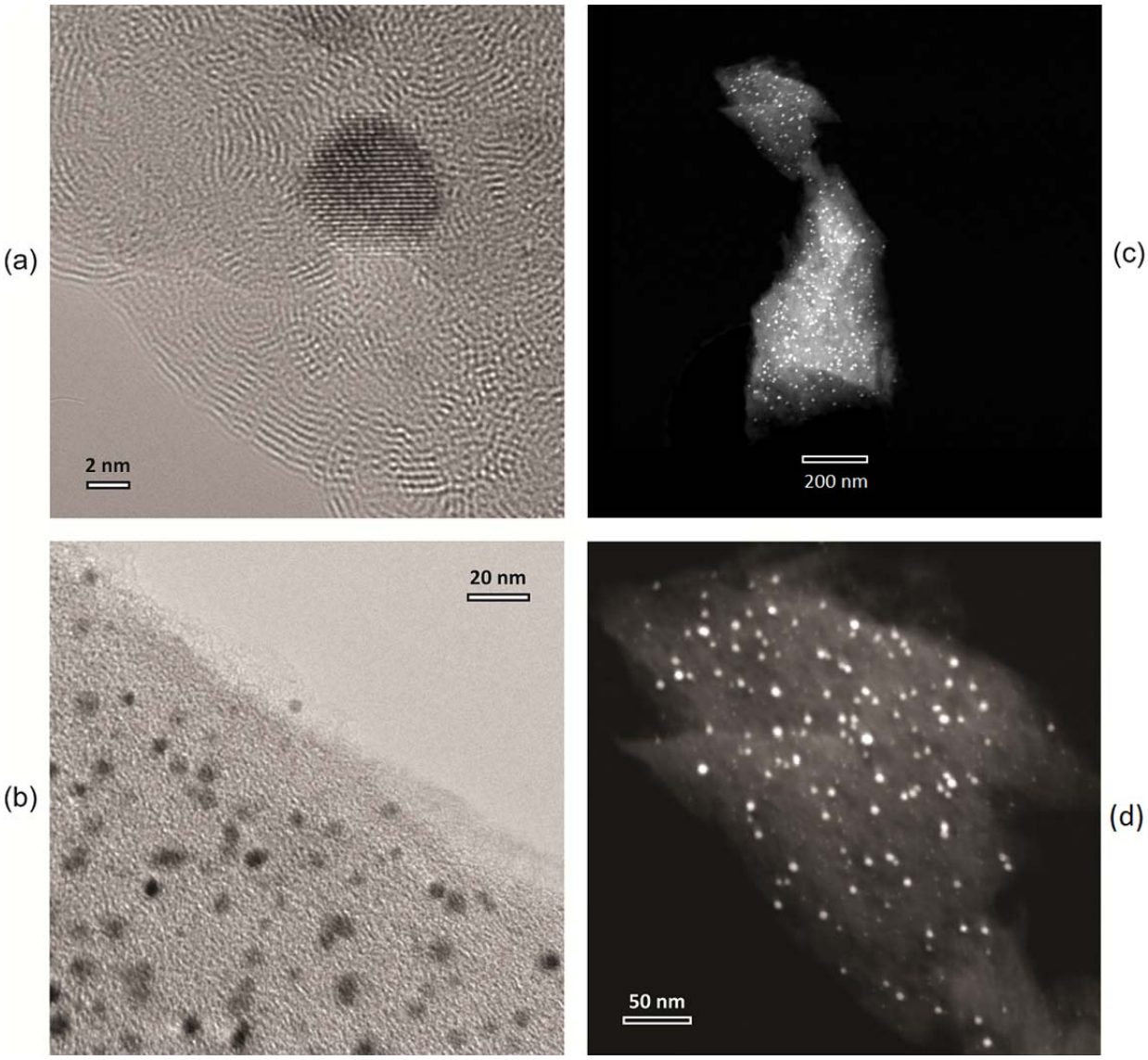

Figure 3.3. TEM micrographs of Pt-MSC-30 at (a) 4753000× and (b) 676600× magnifications. (c) STEM image obtained using a HAADF detector, verifying the successful dispersion of Pt nanoparticles throughout sample. (d) Higher magnification STEM image of an area in (c).

3.3.4 Thermal Gravimetric Analysis

Thermogravimetric analysis (TGA) was performed using a TA Instruments Q500 analyzer with a purge mixture of Ar/air in low flow (20 mL min^{-1}) and normal flow (70 mL min^{-1}) conditions, respectively. The temperature ramp was 10 °C min^{-1} to 100 °C, held at 100 °C for 30 min, then increased 10 °C min^{-1} to 1000 °C and held for 10 min. EDX data

was not consistent from region to region and was not a reliable method to determine the Pt content in Pt-MSC-30. Rather, platinum content was resolved from TGA data which showed a marked loss of mass between 375-415 °C, presumably oxidation of the organic components. The remaining mass at 1000 °C was attributed entirely to platinum and was 7.4% of the total. This value is less than the value of 12% predicted by stoichiometry for the synthesis.

3.4 Hydrogen Sorption

3.4.1 Experimental Methods

Hydrogen uptake isotherms were measured using a volumetric Sieverts apparatus. The system was leak tested over 1-20 h steps up to 7 MPa and showed a maximum leak rate of 1.4×10^{-5} mol h^{-1} of H_2. If fitted to an exponential decay function,

$$n(t) = n_0 \, \mathrm{e}^{-\mathrm{k}\,\mathrm{t}}$$

Equation 3.1

where k is the leak rate, this corresponds to a maximum leak of $k \sim 10^{-8}$ s^{-1} which is negligible for short time measurement.[20] The total volume of the apparatus, depending on the pressure gauge and sample holder selected, was 50-80 mL. The true volume of the sample was subtracted from the empty volume of the sample holder using a skeletal density of 2.1 g mL^{-1} measured by helium expansion. Hydrogen was exposed to the sample at incrementally higher pressures over the course of each isotherm in uniform equilibration steps, ranging from 0.5-24 h per step in different experiments. The system was not returned to vacuum in between steps and the measured hydrogen uptake was

cumulative from step to step. Hydrogen desorption was measured by an analogous method. The sample was evacuated to <1 mPa at room temperature between cycles.

3.4.2 Long-Duration Experiments

To measure the magnitude of the spillover effect at room temperature, unusually long measurements were necessary, sometimes exceeding 1 week in total duration. Even modest pressure (0.1-3 MPa) adsorption measurements of over 12 h duration showed significant scatter in all samples smaller than 0.5 g. Leakage, pressure history, and background adsorption were investigated. It was found that background adsorption in the empty sample holder at room temperature over long steps was comparable to the total uptake measured in 0.2 g samples. Equilibration time between isotherm steps and number of steps were varied to analyze these effects. Increasing the number of adsorption points and the duration of time for equilibration at each point significantly affected measured uptake, for measurements both with and without sample. The most effective approach to minimizing effects of background adsorption was to increase sample mass. It has been recommended that to avoid numerous pitfalls of hydrogen sorption experiments on carbon materials,[20, 21] a sample mass >1 g is best.

A custom-designed 20 mL sample holder was obtained for spillover measurements, accommodating approximately 3 g of sample. This allowed for significant increase in signal due to larger samples, but only a small increase in background. Of course, it is always necessary to subtract a unique background of empty sample holder adsorption from each isotherm measurement of a sample using the same number of isotherm points at roughly the same pressures and with identical technique.

3.4.3 Hydrogen Cycling

High-pressure hydrogen adsorption/desorption cycles were performed for multiple gram quantities of both MSC-30 and Pt-MSC-30, and are shown in Figures 3.4 and 3.5. Hydrogen uptake and delivery were identical after many cycles for MSC-30. Hydrogen uptake capacity for MSC-30 at room temperature and 7 MPa was 3.2 mmol g^{-1} (0.64 wt%). Using the same sample and degassing under vacuum at room temperature for 20 min between cycles, the standard deviation in this value was 0.0003 wt%. Complete desorption to 0.00 wt% at 0 MPa was achieved, with a standard deviation of 0.0006 wt%. Reloading the sample and performing the same adsorption/desorption cycles resulted in combined data which had a standard deviation of 0.003 wt%. This suggests that errors in determining the mass of the dried sample after cycling contributed to a small scatter in the data of different samples, a value within the bounds of usual experimental error.

Hydrogen uptake capacity in Pt-MSC30 was found to change on cycling. It was greatest during the first cycle (after degassing at 623 K under vacuum): 2.6 mmol g^{-1} (0.53 wt%) at 7 MPa and room temperature. Upon desorption, a hysteresis was observed. The desorption curve was extrapolated to 0 MPa, yielding a value of 0.02 wt% which could not be desorbed at room temperature for the first cycle. Using the same sample and degassing under vacuum at room temperature for 20 min between cycles, the uptake capacity at 7 MPa decreased to 0.52 wt% for subsequent cycles. Desorption under these conditions was possible to 0.02 wt% at 0 MPa in all cycles. If the sample is

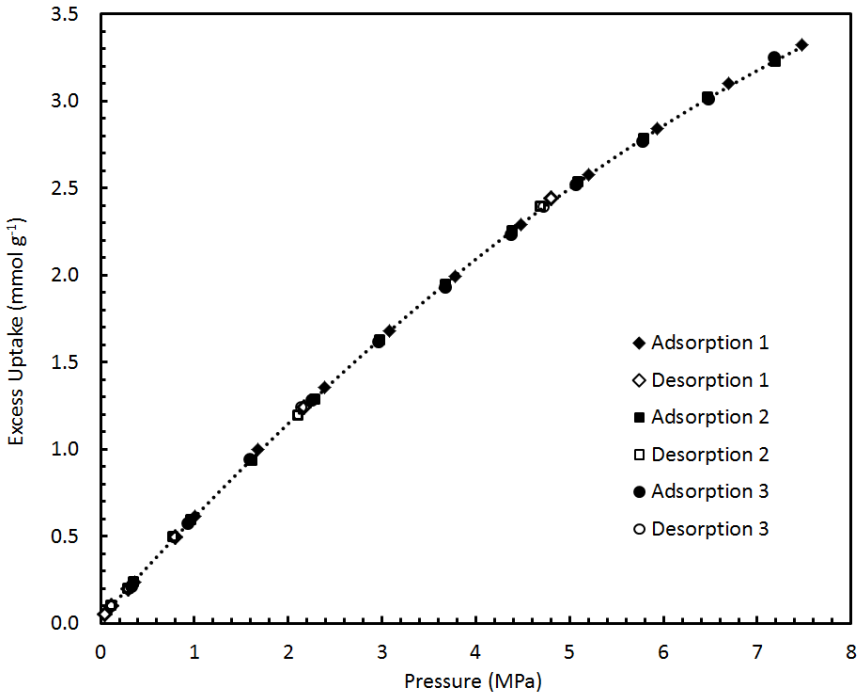

Figure 3.4. Equilibrium adsorption/desorption isotherms of H_2 on MSC-30 at 296 K during three consecutive cycles between 0-8 MPa.

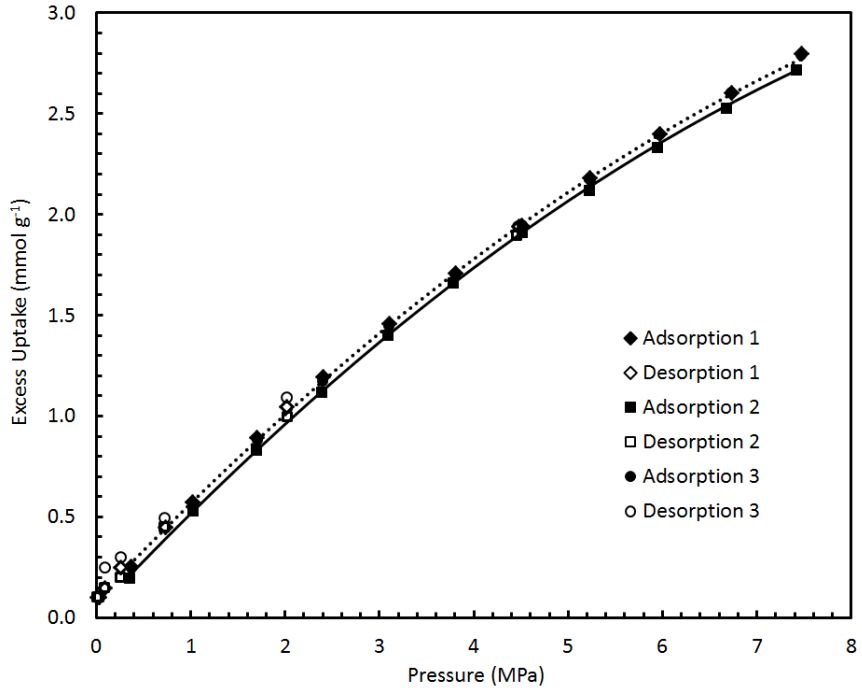

Figure 3.5. Equilibrium adsorption/desorption isotherms of H_2 on Pt-MSC-30 at 296 K during three consecutive cycles between 0-8 MPa.

instead degassed for 8 h between cycles, uptake at 7 MPa is again 0.53 wt%. The amount remaining after desorption is approximately equal to the amount chemisorbed by Pt-MSC-30 at low pressure (0-0.1 MPa). This implies that some hydrogen remains chemisorbed on the surface of the Pt nanoparticles during degassing after short times, but can be removed by evacuating the sample under vacuum overnight.

In the low-pressure regime hydrogen uptake data are collected by a high resolution pressure manometer that is then blocked off for measurements above 0.1 MPa. It can be seen that the high resolution data are consistent with the high-pressure data for large (~3 g) samples in Figure 3.6. Together, the data are used to interpolate the point of intersection of the two isotherm curves.

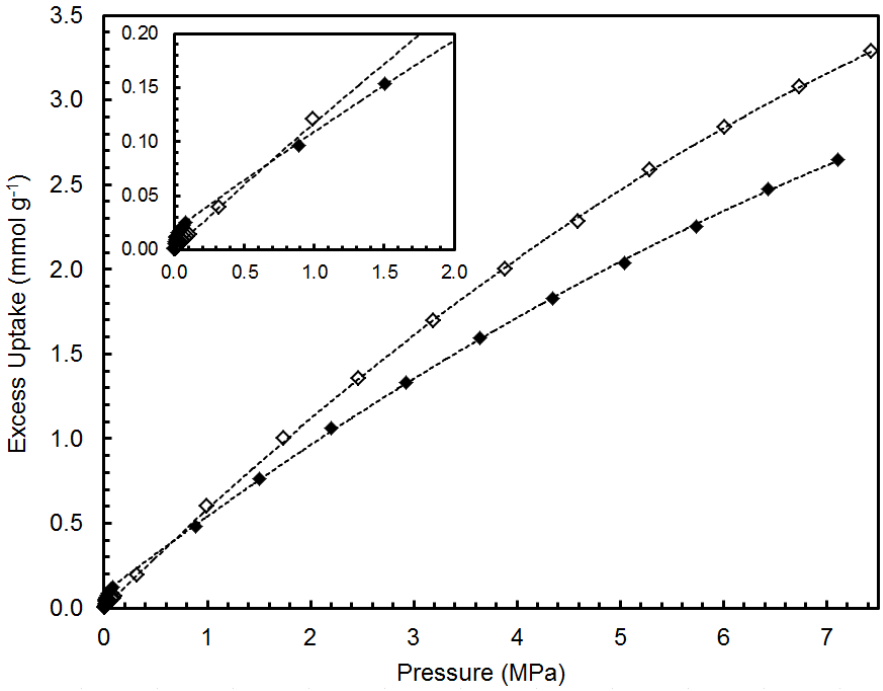

Figure 3.6. Fitted equilibrium adsorption isotherms for MSC-30 and Pt-MSC-30 at 296 K. The data is interpolated to intersect at 0.7 MPa and 0.08 wt%.

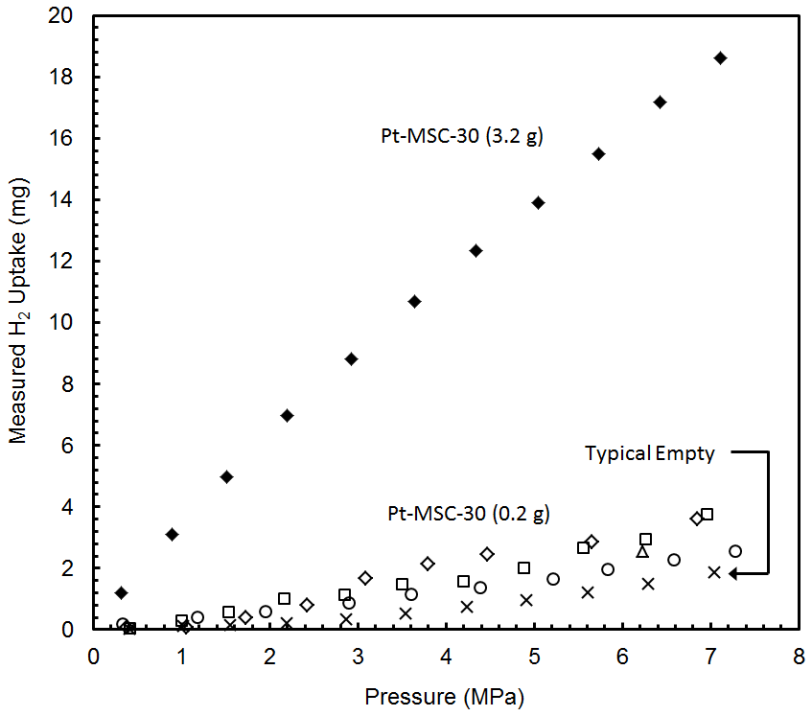

Figure 3.7. Equilibrium adsorption isotherms of H_2 on Pt-MSC-30 samples of varying mass compared to background adsorption by the empty sample holder (containing an aluminum blank) at 296 K. Uptake is shown in units of mass of H_2 detected as missing from the gaseous state, or "adsorbed" by the system.

3.4.4 Hydrogen Sorption Results

Hydrogen uptake isotherms were measured for MSC-30 and Pt-MSC-30 at room temperature, varying the sample size from 0.2-3.4 g. Similar isotherm measurements for aluminum blanks of comparable volume (0.1-1.5 mL) were used to determine the background adsorption of the empty sample holder. A comparison of measured hydrogen uptake (in mg H_2) as a function of pressure is shown for Pt-MSC-30 and an empty sample holder in Figure 3.7. In measurements with small samples (0.2 g), adsorption equilibrium was difficult to determine as room temperature fluctuations continued to slowly change pressure readings even after 60 minutes. Therefore,

equilibration step durations between 0.5-24 h were performed, and results compared. The room temperature isotherm data for small samples of Pt-MSC-30 showed uptake varying from 2.5-3.7 mg H_2 at 7 MPa with larger apparent uptake for longer time of measurement. Temperature changes of even 1 °C over the course of an isotherm step were also found to be highly correlated with large apparent uptake during that step. The problem may originate with the small temperature dependence of the pressure readings. This becomes a very important error for small samples at room temperature where the resolution of the pressure measurement has an important effect on the very small amount of uptake calculated. Hydrogen uptake in 0.2 g samples was a factor of 2 greater than the empty sample holder (background), but variations were also of this order (see Figure 3.7). In samples of mass >3 g, uptake was a factor of 10 greater than background and showed smooth curvature over the course of the experiment despite fluctuations in temperature.

Hydrogen uptake isotherms for large samples (>3 g) of Pt-MSC-30 and unmodified MSC-30 at room temperature, corrected for empty sample holder adsorption, are shown in Figure 3.8. Equilibrium was reached in less than 60 min between each isotherm step and was easily distinguished from continued adsorption. In pure MSC-30, the isotherm showed constant uptake as a function of pressure between 0-2 MPa. At pressures above 2 MPa, the slope decreased. At 6.7 MPa, hydrogen uptake in MSC-30 was 3.1 mmol g^{-1}, consistent with reported values for MSC-30 to within 0.3 mmol g^{-1}.[22, 23] This value was reproducible upon cycling to well within experimental error, to which we assign an upper bound of ±0.05 mmol g^{-1}. In Pt-MSC-30, low-pressure data showed a

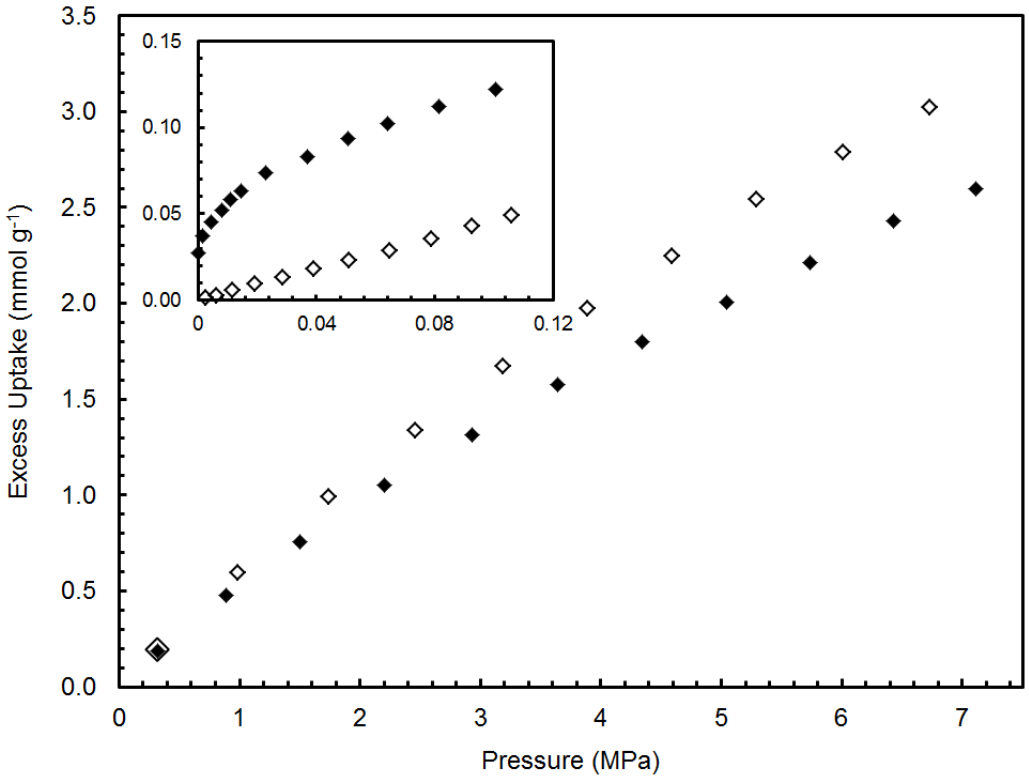

Figure 3.8. Equilibrium adsorption isotherms of H_2 on MSC-30 and Pt-MSC-30 at pressures up to 7 MPa at 296 K. Uptake is shown for large samples (>3 g).

steep initial uptake of hydrogen between 0-0.01 MPa and then a similar constant slope region to MSC-30 between 0.04-2 MPa. The slope of the isotherm in Pt-MSC-30 also decreased slowly at pressures above 2 MPa. Hydrogen uptake at 7.1 MPa was 2.7 mmol g^{-1} in the Pt containing sample on the first adsorption cycle, lower than for the unmodified MSC-30. This value decreased by up to 0.05 mmol g^{-1} in subsequent adsorption cycles. Interpolated hydrogen uptake values at 7 MPa are summarized in Table 3.1.

Table 3.1: BET surface areas (SA) and hydrogen uptake capacities reported for MSC-30, Pt-MSC-30, a similarly prepared Pt doped superactivated carbon, Pt/AX-21, and its precursor, AX-21.

Material	BET SA† (m^2g^{-1})	H_2 Uptake‡ (mmol g^{-1})
MSC-30 [4]	2680	2.8-2.9
MSC-30 [5]	3250	3.0
MSC-30 *	3420	3.2
Pt-MSC-30 *	2810	2.6
AX-21 [8]	2880	2.5
Pt/AX-21 [8]	2518	4.5

* From this study. † Measured using N_2 at 77 K. ‡ Measured using H_2 at 300 K and 7 MPa.

3.5 Discussion

In pure MSC-30 at room temperature, the uptake of hydrogen showed Henry's law behavior in the low-pressure region as expected for low coverage physisorption on activated carbon. The Henry's law constant was 0.1 kg kg^{-1} MPa^{-1} at 296 K. The steep hydrogen uptake between 0-0.01 MPa in Pt-MSC-30 indicated very favorable initial chemisorption of hydrogen onto Pt nanoparticle surface sites. After these sites were filled, Henry's law physisorption of H_2 on the carbon surface occurred in Pt-MSC-30 as in unmodified MSC-30. The Henry's law constant for this physisorptive region was also found to be 0.1 kg kg^{-1} MPa^{-1} at 296 K, suggesting that the same adsorption mechanism is responsible for uptake in both the Pt-containing and unmodified samples at pressures above 0.01 MPa. As pressure increased, the slopes of both isotherms decreased from the Henry's law value due to increased interactions between adsorbed molecules. In Pt-MSC-30, this effect was more apparent because of the additional mass of the platinum.

At 0.7 MPa, the H_2 uptake isotherms intersected at 0.4 mmol g^{-1}. Similar results were also reported for Pd particles on a lower surface area Maxsorb variant.[24]

The addition of Pt nanoparticles to MSC-30 affects only the initial chemisorption at low pressure. The reduced uptake for the room temperature Pt-MSC-30 system at 7 MPa can be readily estimated by making the assumption that the individual contributions of the heavier Pt particle mass (7.4% of the sample) and reduced surface area carbon support (linearly rescaled) were simply additive. In this way, the H_2 uptake was calculated to be 2.5 mmol g^{-1}, close to the measured value. The difference between these values is attributed to a small amount of hydrogen chemisorbed on the surface of the Pt particles.

Spillover has been reported to dramatically enhance H_2 uptake in a similar system, Pt/AX-21, at room temperature, high pressure, and for 0.2 g samples over long (~1 h) equilibration steps between isotherm points.[3] All of these conditions risk substantial error accumulation using a standard Sieverts apparatus. Importantly, the sources of this error (leaks, temperature fluctuations, pressure hysteresis, and empty sample holder adsorption) are expected to cause an apparent *increase* in measured uptake, as opposed to a decrease. Small samples (0.2 g) of Pt-MSC-30 used in this study showed varying hydrogen uptake capacities in different experiments depending on the time allowed for equilibration, up to ±0.6 mg H_2 at 7 MPa and 296 K. Error of this magnitude may normally not be encountered at low (cryogenic) temperature and short equilibration time, or simply ignored when overall uptake mass is much higher in the material. However, for 0.2 g samples of Pt-MSC-30, this contributed an error in reported

uptake of ±1.5 mmol g^{-1} at 7 MPa and 296 K; this error is unacceptably high when the total uptake is 3.0 mmol g^{-1}.

Experiments that require adsorption measurements of carbonaceous materials at room temperature over relatively long equilibration steps must utilize large sample masses to remedy these errors. The same error of ±0.6 mg H_2 at 7 MPa and 296 K observed for a 3.2 g sample of Pt-MSC-30 is a factor of ten smaller in specific uptake (mmol g^{-1}), contributing a possible increase in measured uptake of up to 0.1 mmol g^{-1}. In large sample experiments, after an initial chemisorption at low pressure, platinum served only to increase the total mass of the sample and decrease available surface area for physisorption, thereby effecting a lower specific uptake of H_2 at high pressures.

3.6 Conclusions

If spillover occurred during hydrogen uptake in Pt-MSC-30, it was below the detection limit of volumetric gas adsorption experiments. The upper bound on the amount of hydrogen that participates in spillover is 0.005 mmol g^{-1} which is outside of the accuracy of storage capacity measurements and is not a substantial enhancement for practical applications. The presence of Pt particles on superactivated carbon proved ineffective for increasing hydrogen uptake by spillover. After a small chemisorption at pressures below approximately 0.1 MPa, the platinum served to increase the overall mass of the material and decrease the available surface area, thereby decreasing the overall capacity. Further studies of spillover, and a response to this work, is given in Appendix B.

3.7 References

(1) J. A. Schwarz, U.S. Patent 4,716,736 (1988).

(2) A. D. Lueking and R. T. Yang, 'Hydrogen spillover to enhance hydrogen storage – study of the effect of carbon physicochemical properties', *Appl. Catal., A,* **265**, 259-68 (2004).

(3) Y. Li and R. T. Yang, 'Hydrogen storage on platinum nanoparticles doped on superactivated carbon', *J. Phys. Chem. C,* **111**, 11086-94 (2007).

(4) Y. Li and R. T. Yang, 'Hydrogen storage in metal-organic frameworks by bridged hydrogen spillover', *J. Am. Chem. Soc.,* **128**, 8136-37 (2006).

(5) C. I. Contescu, C. M. Brown, Y. Liu, V. V. Bhat, and N. C. Gallego, 'Detection of hydrogen spillover in palladium-modified activated carbon fibers during hydrogen adsorption', *J. Phys. Chem. C,* **113**, 5886-90 (2009).

(6) D. Saha and S. Deng, 'Hydrogen adsorption on ordered mesoporous carbons doped with Pd, Pt, Ni, and Ru', *Langmuir,* **25**, 12550-60 (2009).

(7) M. Zieliński, R. Wojcieszak, S. Monteverdi, M. Mercy, and M. M. Bettahar, 'Hydrogen storage in nickel catalysts supported on activated carbon', *Int. J. Hydrogen Energy,* **32**, 1024-32 (2007).

(8) A. J. Robell, E. V. Ballou, and M. Boudart, 'Surface diffusion of hydrogen on carbon', *J. Phys. Chem.,* **68**, 2748-53 (1964).

(9) S. T. Srinivas and P. K. Rao, 'Direct observation of hydrogen spillover on carbon-supported platinum and its influence on the hydrogenation of benzene', *J. Catal.,* **148**, 470-77 (1994).

(10) W. C. Conner and J. L. Falconer, 'Spillover in heterogeneous catalysis', *Chem. Rev.,* **95**, 759-88 (1995).

(11) J. C. Meyer, C. O. Girit, M. F. Crommie, and A. Zettl, 'Imaging and dynamics of light atoms and molecules on graphene', *Nature,* **454**, 319-22 (2008).

(12) L. Chen, A. C. Cooper, G. P. Pez, and H. Cheng, 'Mechanistic study on hydrogen spillover onto graphitic carbon materials', *J. Phys. Chem. C,* **111**, 18995-9000 (2007).

(13) A. K. Singh, M. A. Ribas, and B. I. Yakobson, 'H-spillover through the catalyst saturation: an ab initio thermodynamics study', *ACS Nano,* **3**, 1657-62 (2009).

(14) G. M. Psofogiannakis and G. E. Froudakis, 'DFT study of the hydrogen spillover mechanism on Pt-doped graphite', *J. Phys. Chem. C,* **113**, 14908-15 (2009).

(15) A. N. Wennerberg and T. M. O'Grady, U.S. Patent 4,082,694 (1978).

(16) R. T. Yang, *Adsorbents: fundamentals and applications*, John Wiley & Sons, Inc. (2003).

(17) L. Wang, F. H. Yang, R. T. Yang, and M. A. Miller, 'Effect of surface oxygen groups in carbons on hydrogen storage by spillover', *Ind. Eng. Chem. Res.,* **48**, 2920-26 (2009).

(18) T. Otowa, Y. Nojima, and T. Miyazaki, 'Development of KOH activated high surface area carbon and its application to drinking water purification', *Carbon,* **35**, 1315-19 (1997).

(19) J. I. Langford and A. J. C. Wilson, 'Scherrer after sixty years: a survey and some new results in the determination of crystallite size', *J. Appl. Crystallogr.,* **11**, 102-13 (1978).

(20) T. Kiyobayashi, H. T. Takeshita, H. Tanaka, N. Takeichi, A. Züttel, L. Schlapbach, and N. Kuriyama, 'Hydrogen adsorption in carbonaceous materials – how to determine the storage capacity accurately', *J. Alloys Compd.,* **330-332**, 666-69 (2002).

(21) G. G. Tibbetts, G. P. Meisner, and C. H. Olk, 'Hydrogen storage capacity of carbon nanotubes, filaments, and vapor-grown fibers', *Carbon,* **39**, 2291-301 (2001).

(22) H. Nishihara, P. X. Hou, L. X. Li, M. Ito, M. Uchiyama, T. Kaburagi, A. Ikura, J. Katamura, T. Kawarada, K. Mizuuchi, and T. Kyotani, 'High-pressure hydrogen storage in zeolite-templated carbon', *J. Phys. Chem. C,* **113**, 3189-96 (2009).

(23) Y. Kojima, Y. Kawai, A. Koiwai, N. Suzuki, T. Haga, T. Hioki, and K. Tange, 'Hydrogen adsorption and desorption by carbon materials', *J. Alloys Compd.,* **421**, 204-08 (2006).

(24) A. Ansón, E. Lafuente, E. Urriolabeitia, R. Navarro, A. M. Benito, W. K. Maser, and M. T. Martínez, 'Hydrogen capacity of palladium-loaded carbon materials', *J. Phys. Chem. B,* **110**, 6643-48 (2006).